PAPER: Biological modelling and information

On the stationary frequency of programmed ribosomal -1 frameshift

G M Schütz

Institute of Complex Systems II, Forschungszentrum Jülich, 52425 Jülich, Germany

E-mail: g.schuetz@fz-juelich.de

Abstract. We present a stochastic model for programmed ribosomal -1 frameshift, triggered by a slippery sequence and a following pseudoknot on the mRNA template, that allows for the exact derivation of the stationary distribution of ribosome positions and for exact analytical calculations of the stationary rate of frameshift, its efficiency and other quantities of interest. We also present the stationary phase diagram as a function of the initiation rate and the density ribosomes that the pseudoknot can support. These observations provide mathematically rigorous evidence for the notion that the density of molecular motors is an important control parameter for the elongation rate in the presence of slippery sequences both in transcription of RNA and translation of proteins.

Keywords: molecular motors, exclusion processes

Contents

1. Introduction

A protein is a linear heteropolymer where neighbouring amino acids are linked by a peptide bond. The particular sequence of amino acids is encoded in mRNA molecules through the sequence of codons, which are triplet of nucleotides (nt's). The synthesis of a protein in a living cell, as directed by an mRNA template, is carried out by ribosomes which can be regarded as molecular machines [1–4] that move along the mRNA and the process of 'reading' the template step by step for the synthesis by the ribosome is referred to as translation. This process is broadly divided into three stages: initiation, elongation and termination. After the initiation of translation, when a ribosome attaches to the start codon, the elongation of the protein by the ribosome takes place such that the addition of each amino acid monomer to the growing protein is accompanied by a forward stepping (translocation) of the ribosome on its mRNA template by one codon. After termination, the fully assembled protein is released from the ribosome which detaches from the mRNA.

During elongation, the 'reading frame' of the ribosome decodes a triplet of nucleotides on the mRNA template and then slides to the next triplet. This reading frame must be maintained faithfully during the course of normal elongation of the protein. However, on many template mRNA strands occurring in nature there are some 'slippery' sequences of nucleotides where a ribosome can lose its grip on its track, resulting in a shift of its reading frame either backward or forward by one or more nucleotides. These processes, which have important biological functions, are referred to as ribosomal frameshift [5, 6]. After suffering a frameshift, the ribosome resumes its operation but decodes the template using the shifted reading frame, thus leading to a context-dependent alteration of the readout of mRNA.

A different kind of slippage may occur in the synthesis of RNA. The RNA is synthesized through transcription by a RNA polymerase (RNAP) which is another molecular machine that reads the genetic message encoded in a template DNA, in a process which follows a roughly similar pattern of initiation, elongation and termination where the addition of a monomeric subunit to the nascent RNA chain is also accompanied by a step-wise movement of the RNAP motor along the template DNA [2–4, 7]. In this process, slippage is not known to occur by a shift of reading frame, but experiments have revealed that there are specific stretches of DNA sequence where the nascent RNA may

undergo multiple slips with respect to the RNAP [6, 8], thus leading to an alteration of the readout of DNA.

What both processes have in common, apart from the step-wise movement of the molecular motor, is the existence of a special slippery sequences on the template molecule (mRNA or DNA resp.) that leads to a faulty read-out and is accompanied by an irregularity of the motion of the molecular motor responsible for the synthesis (ribosome or RNAP resp.) Also in common is the *simultaneous action of many motors* along the same template which thus leads to interaction between neighbouring motors when they are close to each other on the template. This phenomenon is often referred as traffic flow of molecular motors [2, 3]. Understanding the principles followed by nature for encoding and decoding the genetic message would be incomplete without getting insight into the mechanisms that arise through slippage from the interaction between motors that govern this traffic flow.

Pursuing this line of research, it has been shown [9, 10] that the effect on the traffic of an ensemble of RNAP is similar to the effect of ribosomal slippage on the traffic of an ensemble of ribosomes: in both cases, the slippery sequence on the template molecule acts like a static defect that slows down the motion of a motor compared to its free motion away from the slippery sequence and in the absence of other motors. On the other hand, also in both cases, the interaction with other motors slows down the motion of individual motors, be it either through pure steric hard-core interaction [11, 12] or also in the presence of further short-range interaction [13, 14].

It is the purpose of the present work to study the interplay of these two very different mechanisms (of slowing-down by a slippery sequence on the one hand and mutual interactions on the other hand) by introducing an idealized but analytically tractable model which captures both the stochastic nature of the step-by-step movement and the hard-core repulsion of the motors through steric exclusion. In this way we are able to establish mathematically rigorously the notion that the motor density is a generally an important control parameter for the outcome of the synthesis of the product molecule under slippage conditions, both in translation through mRNA and in transcription through RNAP, and also to further illuminate the role of 'traffic jams' of molecular motors caused by a template inhomogeneity.

2. Model

To be concrete, we consider ribosomal frameshift. The most common of this mode of non-conventional translation [15] is a 'programmed' frameshift at a specific location on the mRNA track, thereby producing a 'fusion' protein. The programmed shift of the reading frame backward by a single nucleotide on the mRNA track, often referred to as −1 frameshift, is the main focus of this work. The classic example of such a fusion product of −1 frame shift is the gag–pol fusion protein of the human immunodeficiency virus (HIV) [5, 6]. We ignore position-independent random frame shifts whose rate has been found to be negligibly small.

Programmed −1 frameshift requires two key ingredients: (a) a slippery sequence (usually about seven nucleotides long) on the mRNA, and (b) a downstream secondary structure of the mRNA [16] which is usually a pseudoknot [17, 18] located a few

nucleotides downstream from the slippery sequence. In order to enter the segment of the mRNA template that forms the pseudoknot, a ribosome has to unwind the secondary structure. Consequently, the pseudoknot acts as a roadblock against the forward movement of the ribosome, leading to a slow-down of translation and allowing for a programmed frameshift at the beginning of the slippery sequence[1].

Not every ribosome suffers a frameshift at a given slippery sequence. It is evident that the frequency of such a programmed frameshift is determined by many details that vary from mRNA to mRNA, such as the specific sequence of codons in the slippery segment, by its distance from the downstream pseudoknot, the kinetics of its unfolding and refolding, and other factors that alter the normal free energy landscape of the ribosome, thereby affecting the stability of various intermediate states as well as the kinetics of transitions [5, 6]. Models that have been developed to account for the mechanisms of stimulation, regulation, and control of frameshift, differ, on the one hand, in their hypotheses regarding the sub-step of the mechano-chemical cycle of the ribosome in which the frameshift is assumed to occur, and, on the other hand, in their assumptions on the assumed structural, energetic and kinetic cause of the slippage [20].

Avoiding these largely open problems, we capture the effects of the slippery sequence and the downstream pseudoknot by a physically motivated alteration of the kinetic rates in a reduced minimal stochastic model of the elongation kinetics, following some of the arguments put forward in [10]. The main purpose of this approach is demonstrate how the frequency of ribosomal frameshift *in vivo* depends (a) on the slowing down of the translation due to the unwinding of the pseudoknot and (b) on the hitherto largely neglected collective effect of ribosomes translating along the same mRNA segment in terms of the average separation between ribosomes (or equivalently the mean number density of the ribosomes) on the downstream mRNA track. Experimental studies of frameshift *in vivo* [21] as well as in experiments with synthetic mRNA secondary structures *in vitro* [22] have provided indications for the interplay of the inter-ribosome separation and the kinetics of unwinding of the pseudoknot.

Our reduced model generalizes the totally asymmetric simple exclusion process (TASEP) [23], whose biologically motivated extensions have proved useful in describing key characteristics of the collective motion of molecular motors [24, 25]. In contrast to earlier TASEP-based models for molecular motors [24–35], we follow [10] in so far as we consider individual nucleotides, rather than triplets of nucleotides (codons), as the basic unit of the mRNA track. However, since we have at the back of our mind the generic influence of a slippery sequence on the motion of molecular motors, we disregard all details of the structure and mechano-chemical cycle of the ribosome. As novelty from the modeling perspective, we describe the mRNA track by two interacting TASEPs on parallel lanes, where each lane represents one of the two relevant reading frames. A frameshift thus corresponds to a jump on the adjacent lane. As shown below, this approach allows for an *exact* analytical treatment of the stationary kinetics of translation with programmed frameshift. Moreover, we go beyond the results of [10] by deriving the phase diagram of frameshift-induced phase segregation as a function of the rates of initiation and termination.

---

[1] This slowing down of the molecular motor associated with the slippery sequence, to be investigated below, is what ribosomal frameshift and slippage of the nascent RNA in RNA synthesis have in common, even though via entirely different mechanisms that we do not capture in our idealized model. We also remark that not all types of road blocks on an mRNA can induce frameshift [19].
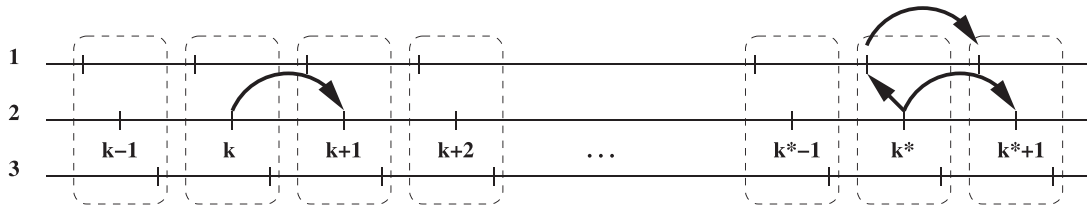
Figure 1. Representation of successive codons k and their three nucleotides on three lanes (α, k) with $\alpha \in \{1, 2, 3\}$. The normal reading frame of the ribosome is represented by lane two, corresponding to jumps from $(2, k) \rightarrow (2, k+1)$ (left). At the special site k^* both normal reading $(2, k^*) \rightarrow (2, k^*+1)$ and frameshift $(2, k^*) \rightarrow (1, k^*)$ can occur, with subsequent reading in the shifted frame $\alpha = 1$ (right). Up to site $k^* - 1$ only lane 2 is required in our model, from site k^* onwards only lanes 1 and 2.

We consider an mRNA in which L successive codons—forming a sequence of $3L$ nucleotides (nt's)—represent the genetic information for a specific amino acid. We label the nt's such that the second (i.e. central) nt in a codon corresponds to the position of the normal reading frame of the ribosome [6]. Each codon (from the start codon 1 to the terminal codon L) is represented as a site k in a linear lattice of three distinct lanes, which represent the sequence of the first, second or third nucleotide in the successive codons respectively. In other words, the $(3(k-1) + \alpha)$th nucleotide of the mRNA that we shall denote by the pair (α, k) is represented by site k in lane α. The total length of the lattice is thus $3L$ in the units of nucleotide length. Since we consider only the −1 frameshift, only the lanes 1 and 2 are relevant for our model (figure 1).

The ribosomes are treated as exclusion particles [25], i.e. each site k can be occupied by at most one particle, thus accounting for the fact that due to steric hindrance a ribosome in its normal reading frame cannot spatially coexist with a ribosome in the shifted reading frame of the same codon. Normal protein synthesis thus proceeds by jumps from positions $(2, k)$ to $(2, k+1)$. The special codon where the ribosomal frameshift is assumed to take place is denoted by k^*.

The next 2–3 nucleotides correspond to the spacer region between the slippery sequence and the pseudoknot while the following nucleotides, corresponding to codons $k^* < k < L'$ with some site $L' < L$, represent the stretch of the mRNA template that is folded in the form of the pseudoknot. A typical value for the length of the length of the mRNA in the pseudoknot is around 40 nt [18]. Since in our model we consider only programmed −1 frameshift at the special site k^*, the first segment of the lattice from site 1 to site $k^* - 1$ has only lane 2, while the remaining lattice from sites k^* up to the terminal site L has two lanes, denoted 2 and 1 respectively. After frameshift, a fusion protein is synthesized by jumps from $(1, k)$ to $(1, k+1)$ for $k \geqslant k^*$.

During the elongation stage a ribosome moves forward by three nucleotides upon successful completion of each elongation cycle. The rate of this translocation in the original (unshifted) frame, i.e., in lane 2, outside the pseudoknot region is captured by an effective rate W of 'hopping' of a ribosome from site k to $k+1$. In principle, the effective rate $W \approx 83 \, \text{s}^{-1}$ [10] can be expressed in terms of the actual rates of the individual transitions among the five distinct mechano-chemical states in the elongation
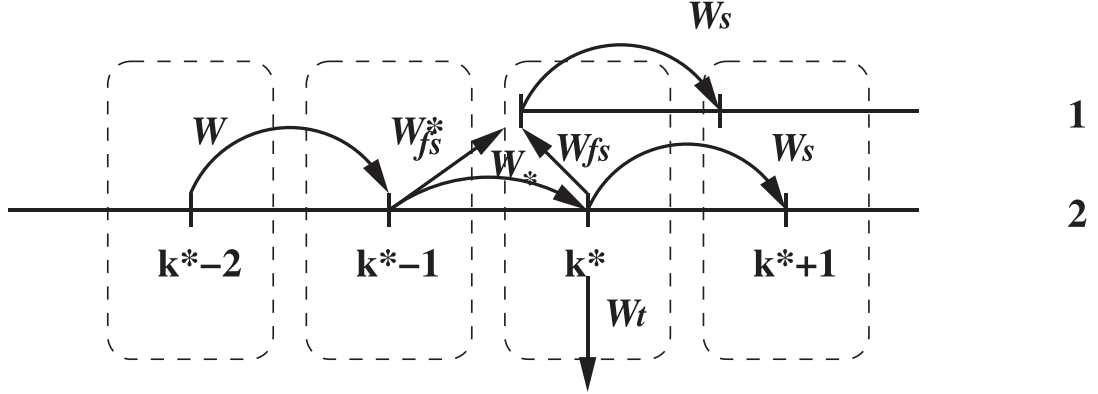
Figure 2. Transitions at the slippery site k^*: normal reading $(2, k^* - 1) \to (2, k^*)$ with rate W_*; reading with frameshift $(2, k^* - 1) \to (1, k^*)$ with rate W_{fs}^* (such that $W_* + W_{\mathrm{fs}}^* = W$ is the normal translocation rate for $k < k^*$); pure frameshift $(2, k^*) \to (1, k^*)$ with rate W_{fs}; premature termination at k^* with rate W_{t}. Inside the pseudoknot region $k \geqslant k^*$ translocation take place with rate $W_{\mathrm{s}} < W$ on both lanes.

stage (for details, see the supplementary information given in arXiv:1605.03434). Here we treat it as a single parameter that sets the time scale of the process (figure 2).

Inside the pseudoknot segment from site k^* to some site $L' < L$ we represent the effective hopping rate in the form.

$$w_{\mathrm{s}} := W_{\mathrm{s}}/W = \exp(-\Delta\tilde{G}_{\mathrm{eff}}) \tag{2.1}$$

where the dimensionless parameter $\Delta\tilde{G}_{\mathrm{eff}} = b\Delta G/(k_{\mathrm{B}}T)$ involves the temperature T, the free energy barrier ΔG that accounts for the necessary unwinding of the pseudoknot by the ribosome, and an effective parameter b that captures the effects of its structural complexity [10]. The phenomenological form (2.1) of the translocation rate has the expected limits $W_{\mathrm{s}} \to W$ when no unwinding is necessary ($\Delta\tilde{G} = 0$) and $W_{\mathrm{s}} \to 0$ for an extremely stiff pseudoknot where $\Delta\tilde{G}$ is large. We shall not make explicit use of (2.1) but treat w_{s} as a variable parameter in the range $0 \leqslant w_{\mathrm{s}} \leqslant 1$.

At the beginning of the slippery sequence around site k^* both frameshift and premature termination can occur. The translocation kinetics depends, as pointed out above, on various structural details of the mRNA. The specific nucleotide $(2, k^*)$ denotes the second nucleotide of the slippery sequence from where the ribosomal frameshift is assumed to take place, corresponding to a translocation of a ribosome to nucleotide $(1, k^*)$, from either from nucleotide $(2, k^*)$ or $(2, k^* - 1)$, the latter process being an effective $+2$ frameshift that leads to the same fusion protein. Thus, in this model the full length of a regular protein (synthesized using the non-shifted frame) and that of a fusion protein consists of the same number of amino acids. We capture this dynamics parametrically by an effective translocation rate W_* from $(2, k^* - 1)$ to $(2, k^*)$ (no frameshift) and W_{fs}^* from $(2, k^* - 1)$ to $(1, k^*)$ (with frameshift), and by a pure frameshift rate W_{fs} from $(2, k^*)$ to $(1, k^*)$ (figure 2).

To fix these rates, we note that since site $k^* - 1$ is not yet part of the slippery sequence, the mean residence time $\tau^* = 1/(W_* + W_{\mathrm{fs}}^*)$ on the nucleotide $(2, k^* - 1)$ is

taken to be equal to the regular mean residence time $\tau = 1/W$ which implies $W_* + W_{\mathrm{fs}}^* = W$. The rate W_{fs} of the −1 frameshift event from $(2, k^*)$ to $(1, k^*)$ depends on the strength of the pseudoknot and on the frequency of breaking the bonds between tRNA and codons. This rate is normally much less than W, so that $w_{\mathrm{fs}} := W_{\mathrm{fs}}/W \ll 1$. However, the frameshift rate is expected to increase with $\Delta \tilde{G}$, i.e., with the stiffness of the pseudoknot. Thus for smaller normalized translocation rate w_{s} in the slippery sequence we assume a larger normalized frameshift rate w_{fs}. In the discussion in section 4 these features are taken into account by the linearized form $w_{\mathrm{fs}} = w_{\mathrm{fs}}^* = 1 - w_{\mathrm{s}}$ of the normalized rates.

The detachment (premature termination) rate W_{t} of a ribosome from the special site k^* is assumed to be of the form

$$w_t := W_{\mathrm{t}}/W = w_{t_0} \exp(-\Delta \tilde{G}'_{\mathrm{eff}}) \tag{2.2}$$

which is motivated by the postulates [10] that (a) in the absence of the pseudoknot (i.e., in the limit $\Delta \tilde{G}'_{\mathrm{eff}} \to 0$ both the forward hopping and premature detachment at the slippery site occur on similar time scales (the ratio being the factor $w_{t_0} < 1$), and that (b) for very stiff pseudoknots (i.e., $\Delta \tilde{G}'_{\mathrm{eff}} \to \infty$ a ribosome practically stalls (no forward movement because $W_{\mathrm{s}} \to 0$) so that there is no possibility of premature detachment. We make no specific assumption on w_{t_0} and $\Delta \tilde{G}'_{\mathrm{eff}}$, but treat w_t as variable parameter in the range $0 \leqslant w_t \leqslant 1 - w_{\mathrm{s}}$.

We note that we make the simplifying assumption that the free energy barrier is independent of the number of ribosomes present in pseudoknot region, even though, as pointed out by an anonymous referee, the presence of ribosomes in that region could reduce this energy barrier.

Translation initiation is captured by the attachment of a ribosome at site $k = 1$ with a rate (i.e., probability per time unit) α. Similarly, termination of translation occurs at site L, both from lane 2 for normal translation and from lane 1 in case of the frameshifted formation of a fusion protein. Since in this work we focus on the effect of the slippery site on ribosome in its environment, i.e., the pseudoknot region $k^*, \ldots, L'$ and the incoming mRNA strand $k < k^*$ and since beyond the pseudoknot ribosome move away with the faster rate $W > W_{\mathrm{s}}$, we ignore ribosome traffic beyond L' in our description. We thus describe leaving the pseudoknot region at L' with an effective rate β.

Denoting by η a configuration of ribosomes on the lattice and by $P(\eta, t)$ the probability of finding η at time t under the Markovian stochastic dynamics described above, the temporal evolution of the probability is given by the master equation

$$\dot{P}(\eta, t) = -\sum_\zeta H_{\eta\zeta} P(\zeta, t) \tag{2.3}$$

where the dot marks the derivative w.r.t. time and H is the negative intensity matrix whose off-diagonal elements $H_{\eta\zeta}$ are the negative transition rates $w_{\eta\zeta}$ from configuration ζ to η and $H_{\eta\eta} = \sum_{\zeta \neq \eta} w_{\zeta\eta}$. Writing the probability distribution as a vector $|P(t)\rangle$, the master equation reads $|\dot{P}(t)\rangle = -H|P(t)\rangle$. The distribution $|\pi\rangle$ satisfying $H|\pi\rangle = 0$ is the stationary distribution of the process from which stationary averages of interest can be calculated. It is convenient to define a configuration η by the two sets of occupation

numbers $n_k \in \{0,1\}$, $1 \leqslant k \leqslant L'$ of ribosomes on lane 2 and $m_k \in \{0,1\}$, $k^* \leqslant k \leqslant L'$ of frameshifted ribosomes on lane 1.

We focus on the effect of the pseudoknot on the upstream translation elongation kinetics at and around the slippery sequence. According to the different processes that occur during translation elongation, the negative bulk intensity matrix H_0 is of the form

$$H_0 = H^{\mathrm{I}} + H^* + H^{\mathrm{fs}*} + H^{\mathrm{fs}} + H^t + H^{\mathrm{II}} \tag{2.4}$$

with the following assignments: H^{I}: translocation in the mRNA segment I before the pseudo knot $(1 \leqslant k < k^*)$, H^*: translocation from $k^* - 1$ to k^* without frameshift, $H^{\mathrm{fs}*}$: translocation from $k^* - 1$ to k^* with frameshift, H^{fs}: -1 frameshift at site k^*, H^t: premature termination at site k^*, H^{II}: translocation in the mRNA segment II inside the pseudoknot $(k^* \leqslant k \leqslant L')$. Initiation at site 1 and normal termination (both from lane 1 and lane 2) at site L are given by negative intensity matrices H^L and H^R resp., so that $H = H_0 + H^L + H^R$ for the full process.

Following the so-called 'quantum Hamiltonian approach' [23] the negative intensity matrices read

$$-H^L = \alpha \left[\sigma_1^- - (1 - \hat{n}_1) \right]$$

$$-H^{\mathrm{I}} = W \sum_{k=1}^{k^*-2} \left[\sigma_k^+ \sigma_{k+1}^- - \hat{n}_k (1 - \hat{n}_{k+1}) \right]$$

$$-H^* = W_* \left[\sigma_{k^*-1}^+ \sigma_{k^*}^- - \hat{n}_{k^*-1} (1 - \hat{n}_{k^*}) \right] (1 - \hat{m}_{k^*})$$

$$-H^{\mathrm{fs}*} = W_{\mathrm{fs}}^* \left[\sigma_{k^*-1}^+ \tau_{k^*}^- - \hat{n}_{k^*-1} (1 - \hat{m}_{k^*}) \right] (1 - \hat{n}_{k^*})$$

$$-H^{\mathrm{fs}} = W_{\mathrm{fs}} (1 - \hat{n}_{k^*-1}) \left[\sigma_{k^*}^+ \tau_{k^*}^- - \hat{n}_{k^*} (1 - \hat{m}_{k^*}) \right]$$

$$-H^t = W_t \left[(\sigma_{k^*}^+ - \hat{n}_{k^*})(1 - \hat{m}_{k^*}) + (\tau_{k^*}^+ - \hat{m}_{k^*})(1 - \hat{n}_{k^*}) \right]$$

$$-H^{\mathrm{II}} = W_{\mathrm{s}} \sum_{k=k^*}^{L'-1} \left[\sigma_k^+ \sigma_{k+1}^- - \hat{n}_k (1 - \hat{n}_{k+1}) \right] (1 - \hat{m}_{k+1})$$

$$+ W_{\mathrm{s}} \sum_{k=k^*}^{L'-1} \left[\tau_k^+ \tau_{k+1}^- - \hat{m}_k (1 - \hat{m}_{k+1}) \right] (1 - \hat{n}_{k+1}) \tag{2.5}$$

$$-H^R = \beta \left[\sigma_{L'}^+ - \hat{n}_{L'} \right] + \beta \left[\tau_{L'}^+ - \hat{m}_{L'} \right]. \tag{2.6}$$

Here σ_k^+ (τ_k^+) annihilates a ribosome at site k of lane 2 (lane 1), while σ_k^- (τ_k^-) creates a ribosome at site k of lane 2 (lane 1). The diagonal matrix $\hat{n}_k$ ($\hat{m}_k$) projects on a ribosome at site k of lane 2 (lane 1).

3. Results

We are interested in the stationary properties of the translation elongation around the slippery sequence.

3.1. Stationary distribution

The first result is the *exact* stationary distribution of the process defined by the negative intensity matrix H with $W_* + W_{\mathrm{fs}}^* = W$. With the parameters

$$z = \frac{1 - w_{\mathrm{s}} - w_t}{w_t} \tag{3.1}$$

$$y_{\mathrm{s}} = \frac{w_{\mathrm{fs}} + w_{\mathrm{fs}}^*}{1 + w_{\mathrm{fs}}} z \tag{3.2}$$

$$z_{\mathrm{s}} = \frac{1 - w_{\mathrm{fs}}^*}{1 + w_{\mathrm{fs}}} z \tag{3.3}$$

and rates of initiation at site 1 and departure at site L' chosen to be

$$\alpha = W \frac{z}{1 + z} \tag{3.4}$$

$$\beta = W_{\mathrm{s}} \frac{1}{1 + z_{\mathrm{s}} + y_{\mathrm{s}}} \tag{3.5}$$

this is the product distribution

$$\pi(\eta) = \frac{1}{(1 + z)^{k^* - 1}(1 + y_{\mathrm{s}} + z_{\mathrm{s}})^{L + 1 - k^*}} \prod_{k=1}^{k^* - 1} z^{n_k} \prod_{k=k^*}^{L} z_{\mathrm{s}}^{n_k} y_{\mathrm{s}}^{m_k} (1 - n_k m_k). \tag{3.6}$$

Notice that the parameters (3.1)–(3.3) play the role fugacities. The factor $(1 - n_k m_k)$ in the probability distribution ensures exclusion of ribosomes at the same site of lanes 1 and 2 due to mutual sterical hindrance.

We stress that no further constraints on the rates of the model (other than the choice (3.4) and (3.5) of the boundary rates) is required for (3.6) to be stationary. The relation $\alpha = (\beta + W_{\mathrm{t}})(y_{\mathrm{s}} + z_{\mathrm{s}})$ that follows from (3.4) and (3.5) is reminiscent of the constraint $\alpha + \beta = 1$ where the standard TASEP with hopping rate 1, injection rate α and detachment rate β has a factorized stationary distribution [36, 37]. We also remark that the factorization property of (3.6) implies that a simple mean field approximation of the model that treats observables at different sites as independent is actually exact, like in the case if the TASEP along the line $\alpha + \beta = 1$. Notice, however, that the two ribosome densities on the same site of lane 1 and 2 resp. in the pseudoknot region (see below) are not independent but highly correlated since $\langle n_k m_k \rangle = 0$ in the stationary distribution.

The stationarity is proved by explicitly verifying $H|\pi\rangle = 0$. In the pseudoknot segment $k \geqslant k^*$ one has

$$\sigma_k^+ |\pi\rangle = z_{\mathrm{s}}(1 - \hat{n}_k - \hat{m}_k)|\pi\rangle \tag{3.7}$$

$$\sigma_k^- (1 - \hat{m}_k)|\pi\rangle = z_{\mathrm{s}}^{-1} \hat{n}_k |\pi\rangle \tag{3.8}$$

$$\tau_k^+ |\pi\rangle = y_{\mathrm{s}}(1 - \hat{m}_k - \hat{n}_k)|\pi\rangle \tag{3.9}$$

$$\tau_k^- (1 - \hat{n}_k)|\pi\rangle = y_{\mathrm{s}}^{-1} \hat{m}_k |\pi\rangle \tag{3.10}$$

$$\sigma_k^+ \tau_k^- |\pi\rangle = \hat{m}_k |\pi\rangle \tag{3.11}$$

$$\hat{n}_k \hat{m}_k |\pi\rangle = 0. \tag{3.12}$$

Inserting these properties into $H|\pi\rangle$ and using the local divergence condition (A.3) proved in the appendix yields

$$-H^L|\pi\rangle = \left[-\alpha + \alpha(1 + z^{-1})\hat{n}_1\right]|\pi\rangle$$

$$-H^{\mathrm{I}}|\pi\rangle = \left(-W\hat{n}_1 + W\hat{n}_{k^*-1}\right)|\pi\rangle, \tag{3.13}$$

$$-H^*|\pi\rangle = \left[-W_*\hat{n}_{k^*-1} + W_*\frac{z}{z_{\mathrm{s}}}\hat{n}_{k^*}\right]|\pi\rangle$$

$$+ \left[W_*\left(1 - \frac{z}{z_{\mathrm{s}}}\right)\hat{n}_{k^*-1}\hat{n}_{k^*} + W_*\hat{n}_{k^*-1}\hat{m}_{k^*}\right]|\pi\rangle, \tag{3.14}$$

$$-H^{\mathrm{fs}*}|\pi\rangle = \left[W_{\mathrm{fs}}^*\frac{z}{y_{\mathrm{s}}}\hat{m}_{k^*} - W_{\mathrm{fs}}^*\hat{n}_{k^*-1}\right]|\pi\rangle$$

$$+ \left[W_{\mathrm{fs}}^*\hat{n}_{k^*-1}\hat{n}_{k^*} + W_{\mathrm{fs}}^*\left(1 - \frac{z}{y_{\mathrm{s}}}\right)\hat{n}_{k^*-1}\hat{m}_{k^*})\right]|\pi\rangle$$

$$-H^{\mathrm{fs}}|\pi\rangle = \left[-W_{\mathrm{fs}}\hat{n}_{k^*} + W_{\mathrm{fs}}\hat{n}_{k^*-1}\hat{n}_{k^*}\right]|\pi\rangle, \tag{3.15}$$

$$-H^t|\pi\rangle = \left[W_{\mathrm{t}}(y_{\mathrm{s}} + z_{\mathrm{s}}) - W_{\mathrm{t}}(1 + y_{\mathrm{s}} + z_{\mathrm{s}})\hat{m}_{k^*} - W_{\mathrm{t}}(1 + y_{\mathrm{s}} + z_{\mathrm{s}})\hat{n}_{k^*}\right]|\pi\rangle, \tag{3.16}$$

$$-H^{\mathrm{II}}|\pi\rangle = W_{\mathrm{s}}\left[\hat{n}_{L'} + \hat{m}_{L'} - \hat{n}_{k^*} - \hat{m}_{k^*} - \hat{n}_{k^*}\hat{m}_{k^*})\right]|\pi\rangle, \tag{3.17}$$

$$-H^R|\pi\rangle = \beta(z_{\mathrm{s}} + y_{\mathrm{s}})|\pi\rangle$$

$$- \left[\beta(1 + z_{\mathrm{s}} + y_{\mathrm{s}})\hat{n}_L + \beta(1 + y_{\mathrm{s}} + z_{\mathrm{s}})\hat{m}_L\right]|\pi\rangle. \tag{3.18}$$

In the stationary state all terms proportional to the various occupation numbers must cancel so that $H|\pi\rangle = 0$ which one verifies by lengthy but straightforward algebra, using (3.4) and (3.5).

3.2. Ribosome density

The fugacities (3.2) and (3.1) parametrize the average ribosomal density, which is the expected ribosome occupation number per codon, as follows. In the upstream segment one has density

$$\rho = \frac{z}{1 + z} \tag{3.19}$$

on lane 2. In terms of the normalized rates $w_\bullet = W_\bullet / W$ one obtains from (3.1)

$$\rho = 1 - \frac{w_t}{1 - w_{\mathrm{s}}} \tag{3.20}$$

In the pseudoknot following the slippery segment the density on lane 2 is given by

$$\rho_{\mathrm{s}} = \frac{z_{\mathrm{s}}}{1 + y_{\mathrm{s}} + z_{\mathrm{s}}} = \frac{1 - w_{\mathrm{fs}}^*}{1 + w_{\mathrm{fs}}}\rho \tag{3.21}$$

and the density of ribosomes that have suffered frameshift, i.e., the density on lane 1 reads

$$\sigma_{\mathrm{s}} = \frac{y_{\mathrm{s}}}{1 + y_{\mathrm{s}} + z_{\mathrm{s}}} = \frac{w_{\mathrm{fs}} + w_{\mathrm{fs}}^*}{1 + w_{\mathrm{fs}}}\rho. \tag{3.22}$$

The mean interribosomal distance in units of 3nt in each segment is the inverse density.

3.3. Fluxes and related quantities

In this work we are interested in exact quantitative results for the stationary rate of translation, both normal and after frameshift, and related quantities such as the stationary rate of frameshift and premature termination.

The upstream flux J of ribosomes, which is defined as the average number of ribosomes that pass from codon to the next per unit time, is given by the stationary expectation of the instantaneous translocation current $W n_k(1 - n_k)$ for $k < k^*$. From the stationary distribution (3.6) of the process one obtains

$$J^{\mathrm{up}} = W\rho(1 - \rho) \tag{3.23}$$

with the upstream ribosome density ρ. Because of the factorization of the stationary distribution this *exact* result is the same as one would obtain in a simple mean field theory that neglects all correlations. The steric hindrance that prevents a ribosome to step forward to a still occupied codon leads to the existence of a maximal current (as function of the density) which is in the present model is attained at density 1/2.

The rate of normal elongation is given by the average number of ribosomes per time unit that complete elongation at the terminal site L. Since in the framework of our model there is no premature termination of elongation after passing through the slippery sequence, one can express the rate of normal elongation by the stationary flux J_2^{s} of ribosomes on lane 2 inside the pseudoknot region. This yields $J_2^{\mathrm{s}} = W_{\mathrm{s}}\langle \hat{n}_k(1 - \hat{n}_{k+1} - \hat{m}_{k+1})\rangle$ for $k \geqslant k^*$ one obtains in the stationary distribution

$$J_2^{\mathrm{s}} = W_{\mathrm{s}}\rho_{\mathrm{s}}(1 - \rho) \tag{3.24}$$

Similarly, the rate of fusion protein elongation is given by the stationary flux J_1^{s} of ribosomes on lane 1 inside the pseudoknot region. This yields $J_1^{\mathrm{s}} = W_{\mathrm{s}}\langle \hat{m}_k(1 - \hat{n}_{k+1} - \hat{m}_{k+1})\rangle$ for $k \geqslant k^*$ one obtains

$$J_1^{\mathrm{s}} = W_{\mathrm{s}}\sigma_{\mathrm{s}}(1 - \rho). \tag{3.25}$$

The stationary rate of frameshift R^{fs} is defined as the average number of ribosomes that undergo frameshift per unit time. Thus, R^{fs} is given by

$$R^{\mathrm{fs}} := W_{\mathrm{fs}}^*\langle \hat{n}_{k^*-1}(1 - \hat{n}_{k^*} - \hat{m}_{k^*})\rangle + W_{\mathrm{fs}}\langle (1 - \hat{n}_{k^*-1})\hat{n}_{k^*}\rangle. \tag{3.26}$$

The stationary distribution yields

$$R^{\text{fs}} = W_{\text{fs}}^* \rho(1-\rho) + W_{\text{fs}}\rho_{\text{s}}(1-\rho). \tag{3.27}$$

Analogously, the stationary rate R^{t} of premature termination is the average number of ribosomes that detach from site k^* on either lane per unit time. Thus $R^{\text{t}} = R_1^{\text{t}} + R_2^{\text{t}}$ with

$$R_2^{\text{t}} := W_{\text{t}}\langle \hat{n}_{k^*}\rangle = W_{\text{t}}\rho_{\text{s}} \tag{3.28}$$

$$R_1^{\text{t}} := W_{\text{t}}\langle \hat{m}_{k^*}\rangle = W_{\text{t}}\sigma_{\text{s}}. \tag{3.29}$$

Finally, the stationary non-slip rate R^* is defined to be the average number of ribosomes that pass through the slippery region per unit time without suffering frameshift or premature termination. This quantity is the stationary translocation rate $W_*\langle \hat{n}_{k^*-1}(1 - \hat{n}_{k^*} - \hat{m}_{k^*})\rangle$ given by

$$R^* = W_*\rho(1 - \rho_{\text{s}} - \sigma_{\text{s}}). \tag{3.30}$$

3.4. Density fluctuations

Stationary density fluctuations of the conserved particle number n_M in an interval of length M are captured by the static compressibility $\kappa = (\langle n_M^2\rangle - \langle n_M\rangle^2)/M$ and more generally for more than one conserved particle number n_M^α by the compressibility matrix K with matrix elements $\kappa_{\alpha\beta} = (\langle n_M^\alpha n_M^\beta\rangle - \langle n_M^\alpha\rangle\langle n^\beta\rangle_M)/M$. From the invariant measure one obtains for the upstream segment

$$\kappa = \rho(1-\rho) \tag{3.31}$$

and inside the pseudoknot region

$$\kappa_{11} = \rho_{\text{s}}(1-\rho_{\text{s}}), \quad \kappa_{22} = \sigma_{\text{s}}(1-\sigma_{\text{s}}), \quad \kappa_{12} = -\rho_{\text{s}}\sigma_{\text{s}}. \tag{3.32}$$

The suppression of the variances κ in the upstream segment and κ_{11} and κ_{22} in the pseudoknot region for high enough densities have their origin in the steric hindrance that we model by the exclusion constraint. The negative cross-correlation $\kappa_{12} = \kappa_{21}$ arises from the impossibility to accommodate a regular ribosome and frameshifted ribosome on the same codon.

4. Discussion

As elaborated upon above, we take $w_t = w_{t_0}(1 - w_{\text{s}})$ with $0 < w_{t_0} < 1$ throughout this section. From (3.20) one finds relation $\rho = 1 - w_{t_0}$. By varying the free parameter w_{t_0} one can study the quantities of interest as a function of the upstream density ρ.

First we note that the ribosome density $\rho_{\text{tot}}^{\text{s}}$ in the pseudoknot segment is then, acccording to (3.21) and (3.22), given by

$$\rho_{\text{tot}}^{\text{s}} = \rho \tag{4.1}$$
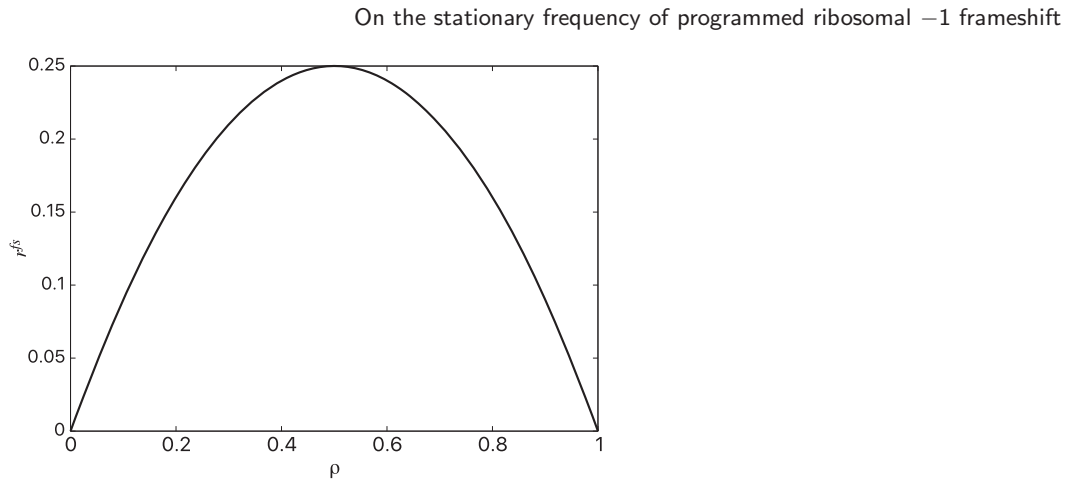
Figure 3. Normalized stationary frameshift rate $r^{\mathrm{fs}} := R_{\mathrm{fs}}/W$ as function of the ribosome density ρ with the choice of amplitude given by $w_{\mathrm{fs}} = w_{\mathrm{fs}}^* = 1$.

despite the loss of ribosomes from premature termination at the slippery sequence. This loss is compensated by the lower translocation rate w_{s} in the pseudoknot region. It follows that the pseudoknot where translocation occurs does not act as a bottleneck.

For the stationary frameshift flux we obtain from the relations (3.2) and (3.3) and from (3.20) and (4.2) In terms of the rates and the upstream density ρ the expression.

$$R^{\mathrm{fs}} = W_{\mathrm{t}} \frac{w_{\mathrm{fs}}^* + w_{\mathrm{fs}}}{(1 - w_{\mathrm{s}})(1 + w_{\mathrm{fs}})} \rho = \frac{w_{\mathrm{fs}}^* + w_{\mathrm{fs}}}{1 + w_{\mathrm{fs}}} J^{\mathrm{up}} = W \frac{w_{\mathrm{fs}}^* + w_{\mathrm{fs}}}{1 + w_{\mathrm{fs}}} \rho (1 - \rho). \qquad (4.2)$$

Using the last equality, we show in figure 3 the variation of the normalized stationary frameshift rate $r^{\mathrm{fs}} = R_{\mathrm{fs}}/W$ with the density ρ. The increase with ρ is expected, but is non-linear which is a consequence of the collective motion of the ribosomes. The mutual exclusion leads to a sublinear growth that has its maximum at $\rho = 1/2$. For higher densities, jamming of ribosomes leads to a decrease of the current and hence of the frameshift rate.

As can be seen from the exact formula (4.2), R_{fs} depends mainly on two factors, (a) the parameters w_{fs} and w_{fs}^* which reflect the complexity of the pseudoknot and (b) the upstream density which indicates the availability ribosomes for frameshift. With decreasing the pseudoknot strength $\Delta \tilde{G}_{\mathrm{eff}}$ the parameter w_{s} increases while $w_t = w_{t_0}(1 - w_{\mathrm{s}})$ (which determines the density) and $w_{\mathrm{fs}}, w_{\mathrm{fs}}^*$ decrease, with the net effect that R_{fs} decreases. The change is monotone since the strongly decreasing product $w_t(w_{\mathrm{fs}}^* + w_{\mathrm{fs}})$ in the amplitude of R^{fs} overcompensates the decrease of R^{fs} due the factor $1 - w_{\mathrm{s}}$ in the denominator. This compensation is readily seen in the second equality where the upstream current that does not depend on w_{s} enters.

A further quantity of interest that characterizes programmed ribosomal frameshift is the fraction ϕ of the proteins synthesized that are a fusion of two proteins 'conjoined at birth'. According to the definitions (3.24) and (3.25) and the results (3.2) and (3.3)
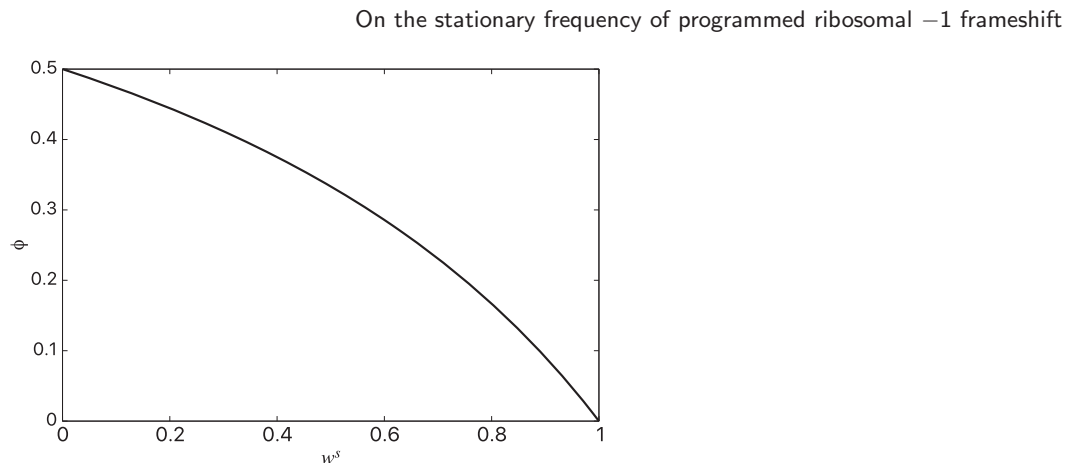
Figure 4. Frameshift efficiency ϕ as function of the normalized translocation rate w_{s} with the choice $w_{\mathrm{fs}} = w_{\mathrm{fs}}^* = 1 - w_{\mathrm{s}}$.

this fraction is given by

$$\phi = \frac{J_1^{\mathrm{s}}}{J_1^{\mathrm{s}} + J_2^{\mathrm{s}}} = \frac{\sigma_{\mathrm{s}}}{\rho} = \frac{w_{\mathrm{fs}}^* + w_{\mathrm{fs}}}{1 + w_{\mathrm{fs}}}. \tag{4.3}$$

It measures the efficiency of the programmed -1 frameshift. As expected, the efficiency vanishes as $w_{\mathrm{s}} \to 1$, corresponding to the absence of a pseudoknot. For decreasing w_{s} the actual rate J_1^{s} of fusion protein production also decreases. However, the normal protein production decreases at the same rate so that the ratio saturates. This is illustrated in figure 4 where the dependence of ϕ on w_{s} is displayed with the choice $w_{\mathrm{fs}} = w_{\mathrm{fs}}^* = (1 - w_{\mathrm{s}})/2$.

Finally, we discuss the phase diagram as function of the initiation rate. In the discussion above it is tacitly assumed that the rates of initiation and termination match the stationary density produced by the slippery sequence in conjunction with the pseudoknot that extends from sites k^* up to a site L'. Then the termination at some site $L > L'$ with rate $\beta^* = W(1 - \rho)$ produces a downstream current $J^{\mathrm{down}} = W\rho(1 - \rho)$ in the segment between the pseudoknot and the termination site L that matches the current $J^{\mathrm{s}} = J_1^{\mathrm{s}} + J_2^{\mathrm{s}}$ in the pseudoknot region, while at the start codon the initiation rate $\alpha^* = W\rho$ produces the same current that matches the stationary upstream value J^{up} (3.23) with J^{s}, thus keeping the pseudoknot segment stationary with the properties discussed above.

However, if initiation at site 1 occurs at a different rate, the situation changes. We focus on the case where $\rho > 1/2$ and a rate of initiation $\alpha = W\rho^L$ with $\rho^L \neq \rho$. For a full discussion of the related problem of the TASEP with a blockage, see [38].

For $\rho^L \neq \rho$ the initiation attempts to produce a current $J^L = W\rho^L(1 - \rho_L)$, which, however, does not match the current $J_{\mathrm{up}} = J^{\mathrm{s}} = J_{\mathrm{down}}$ that keeps the pseudoknot and downstream region stationary. Then, according to the exact solution of the TASEP with open boundaries [36, 37] and, more generally, the theory of boundary-induced phase transition [39], the whole upstream segment $k < k^*$ remains stationary at density ρ as long as $\rho_L > 1 - \rho$, except close to the start codon where the density along the mRNA approaches ρ exponentially fast. At $\rho^L = 1 - \rho$ one has phase coexistence
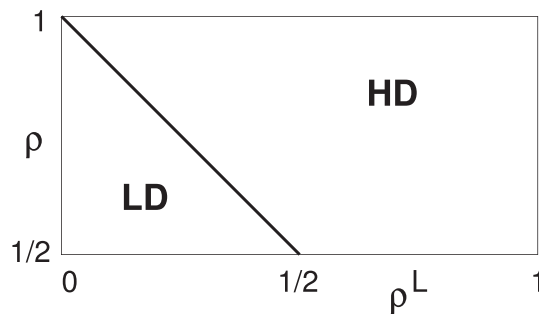
Figure 5. Phase diagram of the mRNA as function of the normalized initiation rate $\rho^L = \alpha/W$ and upstream ribosomal density ρ in the regime $\rho > 1/2$. Phase HD is the high-density phase where the bulk density in the upstream segment $\rho^{\rm up} = \rho$. Phase LD is the low-density phase with $\rho^{\rm up} = \rho^L$, separated from phase 1 by the line $\rho = 1 - \rho^L$ of phase coexistence, corresponding to a first-order non-equilibrium phase transition.

between a low-density domain $1 \leqslant k < k_{\rm s}$ with density $1 - \rho < 1/2$ and a high-density domain $k_{\rm s} < k < k^*$ with density $\rho > 1/2$, analogous to non-equilibrium phase separation in one space dimension [40]. As in the Zel'dovich theory of kinetics of first-order transitions [41], the domain wall motion can be understood as diffusion of the size of the high-density segment with a diffusion coefficient $2D_{\rm s} = \rho(1 - \rho)/(2\rho - 1)$ [42] The high-density segment corresponds to a traffic jam of molecular motors with a fluctuating position of the domain wall which marks the beginning of the jam which is well-understood in systems of finite size [43–47] and For $\rho^L < 1 - \rho$ the domain wall is located in the vicinity of the pseudoknot and the downstream region is stationary a low-density regime with density ρ^L. (figure 5).

With regard to temporal fluctuations we note that the upstream current is the same as for the totally asymmetric simple exclusion process. It follows that collective density waves travel with a speed $v_{\rm c} = 1 - 2\rho$ until they hit either the left boundary or the pseudoknot region. These density fluctuations are known to be in the universality class of the Kardar–Parisi–Zhang (KPZ) equation [48, 49]. In particular, this implies that the density wave broadens in time asymptotically superdiffusively with a power law $t^{2/3}$.

Inside the pseudoknot region there are two conserved densities, one for each lane. Then a richer scenario of potential dynamical universality classes arises, as worked out from non-linear fluctuating hydrodynamics by using mode coupling theory [50, 51] for two conservation laws and later in more detail for an arbitrary number of conservation laws [52]. The crucial ingredients from which the dynamical universality classes are derived are the current-density relation and the compressibility matrix K. Since there are two conservation laws one has two collective density waves. One of the density waves travels with velocity $v_1 = W_{\rm s}(1 - \rho)$, while the other has velocity $v_2 = W_{\rm s}(1 - 2\rho)$, where $\rho = \rho_{\rm s} + \sigma_{\rm s}$. Interestingly, mode coupling theory shows that only one mode belongs to the KPZ universality class and broadens superdiffusively. The second mode is diffusive and broadens with the usual power law $t^{1/2}$.

5. Conclusion

Programmed ribosomal frameshift is one of the most prominent modes of recoding of genetic information. In this paper we have introduced a stochastic model for programmed −1 frameshift for which we have computed the exact stationary solution. This allows for exact analytical calculation of various quantities that highlight the importance of the average ribosome density and of slow translocation rate in a pseudoknot for the rate and efficiency of the frameshift. We have reported quantitative results that demonstrate that the density of ribosomes is an important parameter even when the pseudoknot does not act as an effective bottleneck that would induce a 'traffic jam' of ribosomes [25]. By varying the ribosome density we have illustrated the non-linear effect of the collective ribosome motion on the stationary frameshift rate which exhibits a maximum at intermediate ribosome density $\rho = 1/2$ (figure 3), thus supporting the notion [10] that the ribosome density is an important dynamical control parameter that controls the frequency of programmed ribosomal −1 frameshift. At high densities the suppression of −1 programmed frameshift by a trailing ribosome is similar to the suppression of diffusive backtracking of a RNA polymerase (RNAP) motor by another trailing very closely on a DNA track [53].

The stiffness of the pseudoknot is shown to control monotonically the efficiency of the production of the fusion protein that is synthesized as a result of the frameshift (figure 3) due to an interplay of the reduction of the microscopic frameshift rates and rates of premature termination at the slippery sequence with the density. The relevance of the density as important control parameter emerges also if at high densities $\rho > 1/2$ the rate of initiation attempts to generate an upstream ribosome flux that does not match the current that the pseudoknot with given parameters can support. Then a first-order non-equilibrium phase transition occurs between a phase of low density where the upstream density is given by the (low) initiation rate and phase of high density given by the density ρ that pseudoknot support under stationary conditions. In this phase the upstream density is given by ρ. On the phase transition line both regimes coexist, separated by a sharp diffusing domain wall.

To the best of our knowledge we have reported here the first results for the collective space-time fluctuations of the ribosomal density. Under regular conditions, i.e., without frameshift, density waves travel with finite speed and broaden superdiffusively in the KPZ universality class. Somewhat surprisingly, frameshift leads to second collective mode which does not belong to the generic KPZ class for one-dimensional driven systems, but is diffusive.

In laboratory experiments, the density of the ribosomes on the mRNA can be up- or down-regulated by several different signals and pathways, in particular, by inhibiting initiation at the start codon, which would thus allow for testing the existence of the predicted first-order phase transition. The stiffness of a pseudoknot can be varied artificially [22]. Using such synthetic mRNA strands our theoretical prediction can be tested experimentally by a combination of ribosome profiling technique [54, 55] (for measuring the ribosome density) and FRET (for the frequency of frameshift) [56].

Finally, we point out that the basic mechanisms of the highly idealized model proved rigorously and discussed above are expected to be generic. This corroborates the insight

from RNA transcript slippage [9] that the molecular motor density is generally an important dynamical control parameter for the elongation rate in the presence of slippery sequences on RNA or DNA templates.

Acknowledgments

Appendix A. Local divergence condition for the interacting two-lane TASEP

The two-lane TASEP introduced in this paper is a special case of a more general construction of Markovian multi-lane lattice gas model in which a so-called lattice divergence condition plays a central role [14]. Applying this general construction to the present case yields the following result whose proof we outline since [14] is unpublished at the time of writing the present manuscript.

Proposition A.1. *For $k^* \leqslant k < L$ let*

$$-h_k^{\mathrm{II}} = W_{\mathrm{s}} \left[\sigma_k^+ \sigma_{k+1}^- - \hat{n}_k(1 - \hat{n}_{k+1}) \right] \left[1 + \xi \hat{m}_k + \tilde{\xi} \hat{m}_{k+1} + \varepsilon \hat{m}_k \hat{m}_{k+1} \right]$$
$$+ W_{\mathrm{s}} \left[\tau_k^+ \tau_{k+1}^- - \hat{m}_k(1 - \hat{m}_{k+1}) \right] \left[1 + \tilde{\chi} \hat{n}_k + \chi \hat{n}_{k+1} + \delta \hat{n}_k \hat{n}_{k+1} \right] \quad \text{(A.1)}$$

be the local generator for the two-lane TASEP. For the product measure

$$\pi(\eta) = \prod_{i=k^*}^{L} z_{\mathrm{s}}^{n_i} y_{\mathrm{s}}^{m_i} b^{n_i m_i} \quad \text{(A.2)}$$

the local generator satisfies the local divergence condition

$$-h_k^{\mathrm{II}}|\pi\rangle = W_{\mathrm{s}} \left[\hat{n}_{k+1} + \hat{m}_{k+1} - \hat{n}_k - \hat{m}_k + (\xi + \tilde{\chi})(\hat{n}_{k+1}\hat{m}_{k+1} - \hat{n}_k\hat{m}_k) \right] |\pi\rangle. \quad \text{(A.3)}$$

if and only if the parameter relations

$$\varepsilon = (1 - b)(1 + \tilde{\chi}) \quad \text{(A.4)}$$
$$\delta = (1 - b)(1 + \xi) \quad \text{(A.5)}$$
$$\chi = b(1 + \xi) - 1 \quad \text{(A.6)}$$
$$\tilde{\xi} = b(1 + \tilde{\chi}) - 1 \quad \text{(A.7)}$$

are satisfied.

Proof. We first prove that given the parameter relations the local divergence condition (A.3) follows. For $k^* \leqslant k \leqslant L$ one finds by straightforward computation along the lines of [23]

$$\sigma_k^+ |\pi\rangle = z_{\mathrm{s}}(1 - \hat{n}_k)(1 + (b-1)\hat{m}_k)|\pi\rangle \tag{A.8}$$

$$\sigma_k^- |\pi\rangle = z_{\mathrm{s}}^{-1}\hat{n}_k \left(1 + (b^{-1} - 1)\hat{m}_k\right)|\pi\rangle \tag{A.9}$$

$$\tau_k^+ |\pi\rangle = y_{\mathrm{s}}(1 - \hat{m}_k)(1 + (b-1)\hat{n}_k)|\pi\rangle \tag{A.10}$$

$$\tau_k^- |\pi\rangle = y_{\mathrm{s}}^{-1}\hat{m}_k \left(1 + (b^{-1} - 1)\hat{n}_k\right)|\pi\rangle. \tag{A.11}$$

With the notation $\hat{v}_k = 1 - \hat{n}_k, \hat{u}_k = 1 - \hat{m}_k$ and

$$\hat{f}_k = 1 + \xi\hat{m}_k + \tilde{\xi}\hat{m}_{k+1} + \varepsilon\hat{m}_k\hat{m}_{k+1} \tag{A.12}$$

$$\hat{g}_k = 1 + \tilde{\chi}\hat{n}_k + \chi\hat{n}_{k+1} + \delta\hat{n}_k\hat{n}_{k+1} \tag{A.13}$$

and setting $W_{\mathrm{s}} = 1$ this yields

$$-h_k^{\mathrm{II}}|\pi\rangle = \left\{ \left[\hat{v}_k\hat{n}_{k+1}(\hat{u}_k + b\hat{m}_k)\left(\hat{u}_{k+1} + b^{-1}\hat{m}_{k+1}\right) - \hat{n}_k\hat{v}_{k+1}\right]\hat{f}_k \right.$$
$$\left. + \left[\hat{u}_k\hat{m}_{k+1}(\hat{v}_k + b\hat{n}_k)\left(\hat{v}_{k+1} + b^{-1}\hat{n}_{k+1}\right) - \hat{m}_k\hat{u}_{k+1}\right]\hat{g}_k \right\}|\pi\rangle. \tag{A.14}$$

Now we note

$$\left(\hat{u}_{k+1} + b^{-1}\hat{m}_{k+1}\right)\left(\hat{u}_k + b\hat{m}_k\right)\hat{f}_k$$

$$= \left(\hat{u}_{k+1} + b^{-1}\hat{m}_{k+1}\right)\left[\hat{u}_k + \tilde{\xi}\hat{u}_k\hat{m}_{k+1} + b(1+\xi)\hat{m}_k + b(\tilde{\xi} + \varepsilon)\hat{m}_k\hat{m}_{k+1}\right]$$

$$= \hat{u}_{k+1}\left[\hat{u}_k + b(1+\xi)\hat{m}_k\right]$$

$$\quad + b^{-1}\hat{m}_{k+1}\left[\hat{u}_k + \tilde{\xi}\hat{u}_k + b(1+\xi)\hat{m}_k + b(\tilde{\xi} + \varepsilon)\hat{m}_k\right]$$

$$= \hat{u}_{k+1}\left[1 + \left[b(1+\xi) - 1\right]\hat{m}_k\right]$$

$$\quad + \hat{m}_{k+1}\left[b^{-1}(1+\tilde{\xi}) + \left[(1+\tilde{\xi})(1-b^{-1}) + \xi + \varepsilon\right]\hat{m}_k\right]$$

$$= 1 + \left[b(1+\xi) - 1\right]\hat{m}_k - \hat{m}_{k+1} + \left[1 - b(1+\xi)\right]\hat{m}_k\hat{m}_{k+1}$$

$$\quad + b^{-1}(1+\tilde{\xi})\hat{m}_{k+1} + \left[(1+\tilde{\xi})(1-b^{-1}) + \xi + \varepsilon\right]\hat{m}_k\hat{m}_{k+1}$$

$$= 1 + \left[b(1+\xi) - 1\right]\hat{m}_k + \left[b^{-1}(1+\tilde{\xi}) - 1\right]\hat{m}_{k+1}$$

$$\quad + \left[(1+\tilde{\xi})(1-b^{-1}) + (1+\xi)(1-b) + \varepsilon\right]\hat{m}_k\hat{m}_{k+1}. \tag{A.15}$$

It follows that

$$-h_k^{\mathrm{II}}|\pi\rangle = \left\{\hat{n}_{k+1} + \left[b(1+\xi) - 1\right]\hat{n}_{k+1}\hat{m}_k + \left[b^{-1}(1+\tilde{\xi}) - 1\right]\hat{n}_{k+1}\hat{m}_{k+1}\right.$$

$$+ \left[(1 + \tilde{\xi})(1 - b^{-1}) + (1 + \xi)(1 - b) + \varepsilon \right] \hat{n}_{k+1} \hat{m}_k \hat{m}_{k+1}$$

$$- \hat{n}_k - \xi \hat{n}_k \hat{m}_k - \tilde{\xi} \hat{n}_k \hat{m}_{k+1} - \varepsilon \hat{n}_k \hat{m}_k \hat{m}_{k+1}$$

$$- \hat{n}_k \hat{n}_{k+1} - \left[b(1 + \xi) - 1 \right] \hat{n}_k \hat{n}_{k+1} \hat{m}_k - \left[b^{-1}(1 + \tilde{\xi}) - 1 \right] \hat{n}_k \hat{n}_{k+1} \hat{m}_{k+1}$$

$$- \left[(1 + \tilde{\xi})(1 - b^{-1}) + (1 + \xi)(1 - b) + \varepsilon \right] \hat{n}_k \hat{n}_{k+1} \hat{m}_k \hat{m}_{k+1}$$

$$+ \hat{n}_k \hat{n}_{k+1} + \xi \hat{n}_k \hat{n}_{k+1} \hat{m}_k + \tilde{\xi} \hat{n}_k \hat{n}_{k+1} \hat{m}_{k+1} + \varepsilon \hat{n}_k \hat{n}_{k+1} \hat{m}_k \hat{m}_{k+1}$$

$$+ \hat{m}_{k+1} + \left[b(1 + \tilde{\chi}) - 1 \right] \hat{m}_{k+1} \hat{n}_k + \left[b^{-1}(1 + \chi) - 1 \right] \hat{m}_{k+1} \hat{n}_{k+1}$$

$$+ \left[(1 + \chi)(1 - b^{-1}) + (1 + \tilde{\chi})(1 - b) + \delta \right] \hat{m}_{k+1} \hat{n}_k \hat{n}_{k+1}$$

$$- \hat{m}_k - \tilde{\chi} \hat{m}_k \hat{n}_k - \chi \hat{m}_k \hat{n}_{k+1} - \delta \hat{m}_k \hat{n}_k \hat{n}_{k+1}$$

$$- \hat{m}_k \hat{m}_{k+1} - \left[b(1 + \tilde{\chi}) - 1 \right] \hat{m}_k \hat{m}_{k+1} \hat{n}_k - \left[b^{-1}(1 + \chi) - 1 \right] \hat{m}_k \hat{m}_{k+1} \hat{n}_{k+1}$$

$$- \left[(1 + \chi)(1 - b^{-1}) + (1 + \tilde{\chi})(1 - b) + \delta \right] \hat{m}_k \hat{m}_{k+1} \hat{n}_k \hat{n}_{k+1}$$

$$+ \hat{m}_k \hat{m}_{k+1} + \tilde{\chi} \hat{m}_k \hat{m}_{k+1} \hat{n}_k + \chi \hat{m}_k \hat{m}_{k+1} \hat{n}_{k+1} + \delta \hat{m}_k \hat{m}_{k+1} \hat{n}_k \hat{n}_{k+1} \big\} \, |\pi\rangle$$

$$= \Big\{ \hat{n}_{k+1} + \left[b(1 + \xi) - 1 \right] \hat{n}_{k+1} \hat{m}_k + \left[b^{-1}(1 + \tilde{\xi}) - 1 \right] \hat{n}_{k+1} \hat{m}_{k+1}$$

$$+ \left[(1 + \tilde{\xi})(1 - b^{-1}) + (1 + \xi)(1 - b) + \varepsilon \right] \hat{n}_{k+1} \hat{m}_k \hat{m}_{k+1}$$

$$- \hat{n}_k - \xi \hat{n}_k \hat{m}_k - \tilde{\xi} \hat{n}_k \hat{m}_{k+1} - \varepsilon \hat{n}_k \hat{m}_k \hat{m}_{k+1}$$

$$- \left[b(1 + \xi) - 1 \right] \hat{n}_k \hat{n}_{k+1} \hat{m}_k - \left[b^{-1}(1 + \tilde{\xi}) - 1 \right] \hat{n}_k \hat{n}_{k+1} \hat{m}_{k+1}$$

$$+ \xi \hat{n}_k \hat{n}_{k+1} \hat{m}_k + \tilde{\xi} \hat{n}_k \hat{n}_{k+1} \hat{m}_{k+1}$$

$$- \left[(1 + \tilde{\xi})(1 - b^{-1}) + (1 + \xi)(1 - b) \right] \hat{n}_k \hat{n}_{k+1} \hat{m}_k \hat{m}_{k+1}$$

$$+ \hat{m}_{k+1} + \left[b(1 + \tilde{\chi}) - 1 \right] \hat{n}_k \hat{m}_{k+1} + \left[b^{-1}(1 + \chi) - 1 \right] \hat{n}_{k+1} \hat{m}_{k+1}$$

$$+ \left[(1 + \chi)(1 - b^{-1}) + (1 + \tilde{\chi})(1 - b) + \delta \right] \hat{n}_k \hat{n}_{k+1} \hat{m}_{k+1}$$

$$- \hat{m}_k - \tilde{\chi} \hat{n}_k \hat{m}_k - \chi \hat{n}_{k+1} \hat{m}_k - \delta \hat{n}_k \hat{n}_{k+1} \hat{m}_k$$

$$- \left[b(1 + \tilde{\chi}) - 1 \right] \hat{n}_k \hat{m}_k \hat{m}_{k+1} - \left[b^{-1}(1 + \chi) - 1 \right] \hat{n}_{k+1} \hat{m}_k \hat{m}_{k+1}$$

$$+ \tilde{\chi} \hat{n}_k \hat{m}_k \hat{m}_{k+1} + \chi \hat{n}_{k+1} \hat{m}_k \hat{m}_{k+1}$$

$$- \left[(1 + \chi)(1 - b^{-1}) + (1 + \tilde{\chi})(1 - b) \right] \hat{n}_k \hat{n}_{k+1} \hat{m}_k \hat{m}_{k+1} \Big\} \, |\pi\rangle$$

$$= \Big\{ \hat{n}_{k+1} - \hat{n}_k + \hat{m}_{k+1} - \hat{m}_k$$

$$+ \left[b^{-1}(1 + \tilde{\xi}) - 1 + b^{-1}(1 + \chi) - 1 \right] \hat{n}_{k+1} \hat{m}_{k+1}$$

$$- (\xi + \tilde{\chi}) \hat{n}_k \hat{m}_k$$

$$+ \left[b(1 + \xi) - 1 - \chi \right] \hat{n}_{k+1} \hat{m}_k$$

$$+ \left[b(1 + \tilde{\chi}) - 1 - \tilde{\xi}\right] \hat{n}_k \hat{m}_{k+1}$$

$$+ \left[(2 + \tilde{\xi} + \chi)(1 - b^{-1}) + (1 + \xi)(1 - b) + \varepsilon\right] \hat{n}_{k+1} \hat{m}_k \hat{m}_{k+1}$$

$$- \left[\varepsilon \hat{n}_k + (b - 1)(1 + \tilde{\chi})\right] \hat{n}_k \hat{m}_k \hat{m}_{k+1}$$

$$- \left[\delta + (b - 1)(1 + \xi)\right] \hat{n}_k \hat{n}_{k+1} \hat{m}_k$$

$$+ \left[(2 + \tilde{\xi} + \chi)(1 - b^{-1}) + (1 + \tilde{\chi})(1 - b) + \delta\right] \hat{n}_k \hat{n}_{k+1} \hat{m}_{k+1}$$

$$- \left[(2 + \tilde{\xi} + \chi)(1 - b^{-1}) + (2 + \xi + \tilde{\chi})(1 - b)\right] \hat{n}_k \hat{n}_{k+1} \hat{m}_k \hat{m}_{k+1} \bigg\} |\pi\rangle \quad (A.16)$$

With

$$\varepsilon = (1 - b)(1 + \tilde{\chi}) \tag{A.17}$$

$$\delta = (1 - b)(1 + \xi) \tag{A.18}$$

the action of h_k^{II} on the measure reduces to

$$-h_k^{\mathrm{II}}|\pi\rangle = W_\mathrm{s} \bigg\{ \hat{n}_{k+1} - \hat{n}_k + \hat{m}_{k+1} - \hat{m}_k$$

$$+ \left[b^{-1}(1 + \tilde{\xi}) - 1 + b^{-1}(1 + \chi) - 1\right] \hat{n}_{k+1} \hat{m}_{k+1}$$

$$- (\xi + \tilde{\chi}) \hat{n}_k \hat{m}_k$$

$$+ [b(1 + \xi) - 1 - \chi] \hat{n}_{k+1} \hat{m}_k$$

$$+ \left[b(1 + \tilde{\chi}) - 1 - \tilde{\xi}\right] \hat{n}_k \hat{m}_{k+1}$$

$$+ \left[(2 + \tilde{\xi} + \chi)(1 - b^{-1}) + (2 + \xi + \tilde{\chi})(1 - b)\right] \hat{n}_{k+1} \hat{m}_k \hat{m}_{k+1}$$

$$+ \left[(2 + \tilde{\xi} + \chi)(1 - b^{-1}) + (2 + \xi + \tilde{\chi})(1 - b)\right] \hat{n}_k \hat{n}_{k+1} \hat{m}_{k+1}$$

$$- \left[(2 + \tilde{\xi} + \chi)(1 - b^{-1}) + (2 + \xi + \tilde{\chi})(1 - b)\right] \hat{n}_k \hat{n}_{k+1} \hat{m}_k \hat{m}_{k+1} \bigg\} |\pi\rangle \quad (A.19)$$

With

$$\chi = b(1 + \xi) - 1 \tag{A.20}$$

$$\tilde{\xi} = b(1 + \tilde{\chi}) - 1 \tag{A.21}$$

the last five terms cancel and the local divergence condition (A.3) follows after re-introducing the rate W_s. Since the relations (A.17), (A.18), (A.20), and (A.21), are necessary and sufficient for the cancellation of the unwanted non-divergence terms, also the reverse direction of the derivation is valid. □

Corollary A.2. *With the rates*

$$\hat{f}_k = 1 + \xi \hat{m}_k + [b(1 + \tilde{\chi}) - 1]\hat{m}_{k+1} + (1 - b)(1 + \tilde{\chi})\hat{m}_k \hat{m}_{k+1}$$

$$\hat{g}_k = 1 + \tilde{\chi} \hat{n}_k + [b(1 + \xi) - 1]\hat{n}_{k+1} + (1 - b)(1 + \xi)\hat{n}_k \hat{n}_{k+1} \tag{A.22}$$

the local generator h_k^{II} satisfies the local divergence condition (A.3) for any value of the parameters $\xi, \tilde{\chi}, b$ [57] and for

$$H^{\mathrm{II}} := W_{\mathrm{s}} \sum_{k=k^*}^{L-1} h_k^{\mathrm{II}} \tag{A.23}$$

one has

$$-H^{\mathrm{II}}|\pi\rangle = W_{\mathrm{s}} \left[\hat{n}_L + \hat{m}_L - \hat{n}_{k^*} - \hat{m}_{k^*} + (\xi + \tilde{\chi})(\hat{n}_L \hat{m}_L - \hat{n}_{k^*} \hat{m}_{k^*}) \right] |\pi\rangle. \tag{A.24}$$

Corollary A.3. *For $b = 0$ (at most one particle per site) one has $\varepsilon = 1 + \tilde{\chi}, \delta = 1 + \xi$, $\chi = \tilde{\xi} = -1$ which yields*

$$-h_k^{\mathrm{II}} = W_{\mathrm{s}} \left[\sigma_k^+ \sigma_{k+1}^- - \hat{n}_k(1 - \hat{n}_{k+1}) \right] \left[1 + \xi \hat{m}_k - \hat{m}_{k+1} + (1 + \tilde{\chi}) \hat{m}_k \hat{m}_{k+1} \right]$$
$$+ W_{\mathrm{s}} \left[\tau_k^+ \tau_{k+1}^- - \hat{m}_k(1 - \hat{m}_{k+1}) \right] \left[1 + \tilde{\chi} \hat{n}_k - \hat{n}_{k+1} + (1 + \xi) \hat{n}_k \hat{n}_{k+1} \right]. \tag{A.25}$$

and the local divergence condition reduces to

$$-h_k^{\mathrm{II}}|\pi\rangle = W_{\mathrm{s}} \left[\hat{n}_{k+1} + \hat{m}_{k+1} - \hat{n}_k - \hat{m}_k \right] |\pi\rangle. \tag{A.26}$$

since $\hat{n}_k \hat{m}_k |\pi\rangle = 0$ if $b = 0$.

Remark A.4.

(a) For $\xi = 0, \tilde{\chi} = -1$ one obtains

$$-h_k^{\mathrm{II}} = W_{\mathrm{s}} \left[\sigma_k^+ \sigma_{k+1}^- - \hat{n}_k(1 - \hat{n}_{k+1}) \right] (1 - \hat{m}_{k+1})$$
$$+ W_{\mathrm{s}} \left[\tau_k^+ \tau_{k+1}^- - \hat{m}_k(1 - \hat{m}_{k+1}) \right] (1 - \hat{n}_k)(1 + (b - 1)\hat{n}_{k+1}) \tag{A.27}$$

and

$$-H^{\mathrm{II}}|\pi\rangle = W_{\mathrm{s}} \left[\hat{n}_L + \hat{m}_L - \hat{n}_{k^*} - \hat{m}_{k^*} - (\hat{n}_L \hat{m}_L - \hat{n}_{k^*} \hat{m}_{k^*}) \right] |\pi\rangle \tag{A.28}$$
$$= W_{\mathrm{s}} \left[(1 - \hat{n}_{k^*})(1 - \hat{m}_{k^*}) - (1 - \hat{n}_L)(1 - \hat{m}_L) \right] |\pi\rangle. \tag{A.29}$$

(b) For $b = 0$ and

$$\tilde{\chi} = -(1 + \xi) \tag{A.30}$$

the local generator reduces to

$$-h_k^{\mathrm{II}} = W_{\mathrm{s}} \left[\sigma_k^+ \sigma_{k+1}^- - \hat{n}_k(1 - \hat{n}_{k+1}) \right] (1 + \xi \hat{m}_k)(1 - \hat{m}_{k+1})$$
$$+ W_{\mathrm{s}} \left[\tau_k^+ \tau_{k+1}^- - \hat{m}_k(1 - \hat{m}_{k+1}) \right] (1 - (1 + \xi)\hat{n}_k)(1 - \hat{n}_{k+1}) \quad \text{(A.31)}$$

with $-1 \leqslant \xi \leqslant 0$.

(c) For $b = 1$ (no exclusion between lanes) one has $\varepsilon = \delta = 0, \chi = \xi, \tilde{\xi} = \tilde{\chi}$ which yields

$$-h_k^{\mathrm{II}} = W_{\mathrm{s}} \left[\sigma_k^+ \sigma_{k+1}^- - \hat{n}_k(1 - \hat{n}_{k+1}) \right] [1 + \xi \hat{m}_k + \tilde{\chi} \hat{m}_{k+1}]$$
$$+ W_{\mathrm{s}} \left[\tau_k^+ \tau_{k+1}^- - \hat{m}_k(1 - \hat{m}_{k+1}) \right] [1 + \tilde{\chi} \hat{n}_k + \xi \hat{n}_{k+1}]. \quad \text{(A.32)}$$

This is the two-lane model that exhibits fluctuations in the dynamical Fibonacci-universality classes [52]. Specifically, for $\chi = \xi = \tilde{\xi} = \tilde{\chi} = 0$ one has two decoupled TASEPs which implies the well-known local divergence condition

$$-h_k^{\mathrm{I}}|\pi\rangle = W \left[\hat{n}_{k+1} - \hat{n}_k \right] |\pi\rangle. \quad \text{(A.33)}$$

for the TASEP with the stationary Bernoulli product measure π with fugacity z.

References

[1] Frank J 2010 *Molecular Machines in Biology: Workshop of the Cell* (New York: Cambridge University Press)
[2] Chowdhury D 2013 Stochastic mechano-chemical kinetics of molecular motors: a multidisciplinary enterprises from a physicist's perspective *Phys. Rep.* **529** 1
[3] Chowdhury D 2013 Modeling stochastic kinetics of molecular machines at multiple levels: from molecules to modules *Biophys. J.* **104** 2331
[4] Kolomeisky A B 2013 Motor proteins and molecular motors: how to operate machines at the nanoscale *J. Phys.: Condens. Matter.* **25** 463101
[5] Farabaugh P J 1997 *Programmed Alternative Reading of the Genetic Code* (Berlin: Springer)
[6] Atkins J F and Gesteland R F (ed) 2010 *Recoding: Expansion of Decoding Rules Enriches Gene Expression* (New York: Springer) vol 24
[7] Buc H and Strick T (ed) 2009 *RNA Polymerases as Molecular Motors* (London: The Royal Society of Chemistry)
[8] Turnbough C L 2011 *Curr. Opin. Microbiol.* **14** 142
[9] Ghosh S, Dutta A, Patra S, Sato J, Nishinari K and Chowdhury D 2019 Biologically motivated asymmetric exclusion process: interplay of congestion in RNA polymerase traffic and slippage of nascent transcript *Phys. Rev.* E **99** 052122
[10] Mishra B, Schütz G M and Chowdhury D 2016 Slip of grip of a molecular motor on a crowded track: modeling shift of reading frame of ribosome on RNA template *Europhys. Lett.* **114** 68005
[11] Klumpp S and Hwa T 2008 Stochasticity and traffic jams in the transcription of ribosomal RNA: intriguing role of termination and antitermination *Proc. Natl Acad. Sci. USA* **105** 18159–64
[12] Tripathi T and Chowdhury D 2008 Interacting RNA polymerase motors on a DNA track: effects of traffic congestion and intrinsic noise on RNA synthesis *Phys. Rev.* E **77** 011921
[13] Teimouri H, Kolomeisky A B and Mehrabiani K 2015 Theoretical analysis of dynamic processes for interacting molecular motors *J. Phys. A: Math. Theor.* **48** 065001
[14] Belitsky V and Schütz G M 2019 RNA polymerase interactions and elongation rate *J. Theor. Biol.* **462** 370–80
[15] Firth A E and Brierley I 2012 Stochastic mechano-chemical kinetics of molecular motors: a multidisciplinary enterprises from a physicist's perspective *J. Gen. Virol.* **93** 1385
[16] Kim H K *et al* 2014 A frameshifting stimulatory stem loop destablizes the hybrid state and impedes ribosomal translocation *Proc. Natl Acad. Sci. USA* **111** 5538
[17] Brierley I *et al* 2007 Viral RNA pseudoknots: versatile motifs in gene expression and replication *Nat. Rev. Microbiol.* **5** 598
[18] Giedroc D P and Cornish P V 2009 Frameshifting RNA pseudoknots: structure and mechanism *Virus Res.* **139** 193

[19] Brierley I *et al* 2008 RNA pseudoknots and the regulation of protein synthesis *Biochem. Soc. Trans.* **36** 684

[20] Tinoco I Jr *et al* 2013 Frameshifting dynamics *Biopolymers* **99** 1147

[21] Lopinski J D *et al* 2000 Kinetics of ribosomal pausing during programmed-1 translational frameshifting *Mol. Cell. Biol.* **20** 1095

[22] Tholstrup J *et al* 2012 mRNA psudoknot structures can act as ribosomal roadblocks *Nucleic Acids Res.* **40** 303

[23] Schütz G M 2001 Exactly solvable models for many-body systems far from equilibrium *Phase Transitions and Critical Phenomena* ed C Domb and J Lebowitz (London: Academic Press) vol 19

[24] Chowdhury D *et al* 2005 Physics of transport and traffic phenomena in biology: From molecular motors to cells to organisms *Phys. Life Rev.* **2** 318

[25] Schadschneider A, Chowdhury D and Nishinari K 2011 *Stochastic Transport in Complex Systems: From Molecules to Vehicles* (Amsterdam: Elsevier)

[26] Sharma A K and Chowdhury D 2011 Distribution of dwell times of a ribosome: Effects of infidelity, kinetic proofreading and ribosome crowding *Phys. Biol.* **8** 026005

[27] Sharma A K and Chowdhury D 2011 Stochastic theory of protein synthesis and polysome: ribosome profile on a single mRNA transcript *J. Theor. Biol.* **289** 36

[28] Chou T *et al* 2011 Non-equilibrium statistical mechanics: From a paradigmatic model to biological transport *Rep. Prog. Phys.* **74** 116601

[29] Zia R K P *et al* 2011 Modeling translation in protein synthesis with TASEP: a tutorial and recent developments *J. Stat. Phys.* **144** 405

[30] von der Haar T 2012 Mathematical and computational modelling of ribosomal movement and protein synthesis: an overview *Comput. Struct. Biotechnol. J.* **1** e201204002

[31] Appert-Rolland C *et al* 2015 Intracellular transport driven by cytoskeletal motors: general mechanisms and defects *Phys. Rep.* **593** 1

[32] Chou T and Lakatos G 2004 Clustered bottlenecks in mRNA translation and protein synthesis *Phys. Rev. Lett.* **93** 198101

[33] Lakatos G and Chou T 2003 Totally asymmetric exclusion processes with particles of arbitrary size *J. Phys.* A **36** 2027

[34] Mitarai N and Pedersen S 2013 Control of ribosome traffic by position-dependent choice of synonymous codons *Phys. Biol.* **10** 056011

[35] Turci F *et al* 2013 Transport on a Lattice with Dynamical Defects *Phys. Rev.* E **87** 012705

[36] Schütz G and Domany E 1993 Phase transitions in an exactly soluble one- dimensional asymmetric exclusion model *J. Stat. Phys.* **72** 277–96

[37] Derrida B, Evans M R, Hakim V and Pasquier V 1993 Exact solution of a 1D asymmetric exclusion model using a matrix formulation *J. Phys. A: Math. Gen.* **26** 1493–517

[38] Kolomeisky A B 1998 *J. Phys. A: Math. Gen.* **31** 1153

[39] Kolomeisky A B, Schütz G M, Kolomeisky E B and Straley J P 1998 Phase diagram of one-dimensional driven lattice gases with open boundaries *J. Phys. A: Math. Gen.* **31** 6911–9

[40] Kafri Y, Levine E, Mukamel D, Schütz G M and Willmann R D W 2003 Novel phase-separation transition in one-dimensional driven models *Phys. Rev.* E **68** 035101

[41] Landau L D and Lifshitz E M 1981 *Physical Kinetics (Course of Theoretical Physics 10)* ed E M Lifshitz and L P Pitaevskii (Oxford: Pergamon Press)

[42] Ferrari P A and Fontes L R G 1994 Shock fluctuations in the asymmetric simple exclusion process *Probab. Theor. Relat. Field* **99** 305–19

[43] Schütz G M 1997 The Heisenberg chain as a dynamical model for protein synthesis—Some theoretical and experimental results *Int. J. Mod. Phys.* B **11** 197–202

[44] Derrida B, Lebowitz J L and Speer E 1997 Shock profiles in the asymmetric simple exclusion process in one dimension *J. Stat. Phys.* **89** 135–67

[45] Dudziński M and Schütz G M 2000 Relaxation spectrum of the asymmetric exclusion process with open boundaries *J. Phys.* A **33** 8351–64

[46] Nagy Z, Appert C and Santen L 2002 Relaxation times in the ASEP model using a DMRG method *J. Stat. Phys.* **109** 623–39

[47] de Gier J and Essler F H L 2006 Exact spectral gaps of the asymmetric exclusion process with open boundaries *J. Stat. Mech.* P12011

[48] Halpin-Healy T and Takeuchi K A 2015 A KPZ cocktail-shaken, not stirred *J. Stat. Phys.* **160** 794–814

[49] Spohn H 2017 The Kardar–Parisi–Zhang equation—a statistical physics perspective, Les Houches summer school July 2015 session CIV *Stochastic Processes and Random Matrices* ed G Schehr, A Alexander, Y V Fyodorov, N O'Connell and L F Cugliandolo (Oxford: Oxford University Press)

[50] Popkov V, Schmidt J and Schütz G M 2015 Universality classes in two-component driven diffusive systems *J. Stat. Phys.* **160** 835–60

[51] Spohn H and Stoltz G 2015 Nonlinear fluctuating hydrodynamics in one dimension: the case of two conserved fields *J. Stat. Phys.* **160** 861–84

[52] Popkov V, Schadschneider A, Schmidt J and Schütz G M 2015 Fibonacci family of dynamical universality classes *Proc. Natl Acad. Sci. USA* **112** 12645–50

[53] Sahoo M and Klumpp S 2011 Stochastic kinetics of ribosomes: Single motor properties and collective behavior *Europhys. Lett.* **96** 60004

[54] Ingolia N T 2014 Ribosome profiling reveals pervasive translation outside of annotated protein-coding genes *Nat. Rev. Genet.* **15** 205

[55] Ingolia N T 2016 *Cell* **165** 22

[56] Tinoco I Jr and Gonzalez R L Jr 2011 Biological mechanisms, one molecule at a time *Genes Dev.* **25** 1205

[57] Popkov V and Schütz G M 2003 Shocks and excitation dynamics in a driven diffusive two-channel system *J. Stat. Phys.* **112** 523–40